

# The internal friction and phase transition of solid oxygen

A.I. Erenburg

*Ben-Gurion University of Negev, P.O.B. 653, Beer-Sheva 84105, Israel*

E-mail: erenbura@bgu.ac.il

A.V. Leont'eva, V.N. Varyukhin, G.A. Marinin, and A.Yu. Prokhorov

*Galkin Donetsk Institute for Physics and Engineering of the National Academy of Sciences of Ukraine*

*72 Luxemburg Str., Donetsk 83114, Ukraine*

E-mail: vesta-news@yandex.ru; tonya.leont@gmail.com

Received December 10, 2010

We report an experimental study of the low frequency internal friction (LTIF) in solid oxygen in temperature range 7–52 K. Comparison of the temperature dependence of IF with data of x-ray diffraction and other thermodynamic and elastic properties, shows that anomalies of temperature dependence of the internal friction are resulted from phase transitions in solid oxygen.

PACS: 07.20.Mc Cryogenics; refrigerators, low-temperature detectors, and other low-temperature equipment;  
**62.40.+I** Internal friction;  
**64.70.K**– Solid–solid transition;  
 61.05.cp X-ray diffraction.

Keywords: solid oxygen; low frequency internal friction; solid–solid phase transition; x-ray diffraction in crystal structure.

## Introduction

Solid oxygen is one of the most peculiar crystals of the group of the diatomic molecular crystals. The peculiarity ensues largely due to the fact that the O<sub>2</sub> molecule, in its electronic ground state, has a spin  $S = 1$ . As a result, solid oxygen combines the properties of molecular crystal and magnetic material and undergoes crystalline and/or magnetic transitions.

The solid oxygen exists in three crystalline modifications at equilibrium vapor pressure. Low-temperature monoclinic  $\alpha$ -phase (Fig. 1) has long-range orientational order

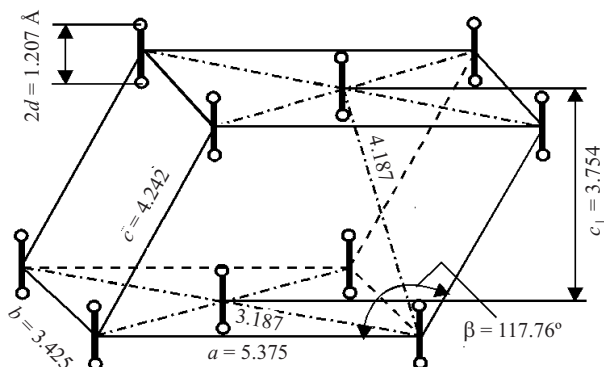


Fig. 1. Crystal structure of  $\alpha$ -O<sub>2</sub> ( $T = 7$  K).

and quasi-two-dimensional antiferromagnetic molecular order [1,2].

A heating of a sample leads to the first phase transition at  $T = 23.88$  K. After the phase transition a rhombohedral  $\beta$ -modification (Fig. 2) of solid oxygen becomes paramagnetic with long-range orientational molecular order in temperature range between  $23.88 \text{ K} \leq T \leq 43.78 \text{ K}$  [1–3].

At high-temperatures the cubic  $\gamma$ -phase (Fig. 3) represents two orientationally disordered molecules and six molecules making a plane rotation.

Table 1. Data of lattice parameter  $\alpha$  and  $\beta$  phases in monoclinic axis at the area  $\alpha \rightarrow \beta$  phase transition ( $T = 23.5$ – $24$  K) [2].

Lattice parameter	$\alpha$ -phase ( $T = 23.5$ K)	$\beta$ -phase ( $T = 24$ K)	$\Delta\alpha\beta, \%$
$a, \text{Å}$	5.408	5.667	+ 4.7
$b, \text{Å}$	3.424	3.272	– 4.6
$c, \text{Å}$	4.254	4.353	–
$c_{\perp}, \text{Å}$	3.762	3.765	+0.8
$\beta, \text{deg}$	117.84	120.12	–
$V, \text{cm}^3/\text{mol}$	20.98	21.02	+1.9

Notes:  $c_{\perp} = c \sin \beta$

More detail investigation of these phase transitions designates a different nature of structure transformations.

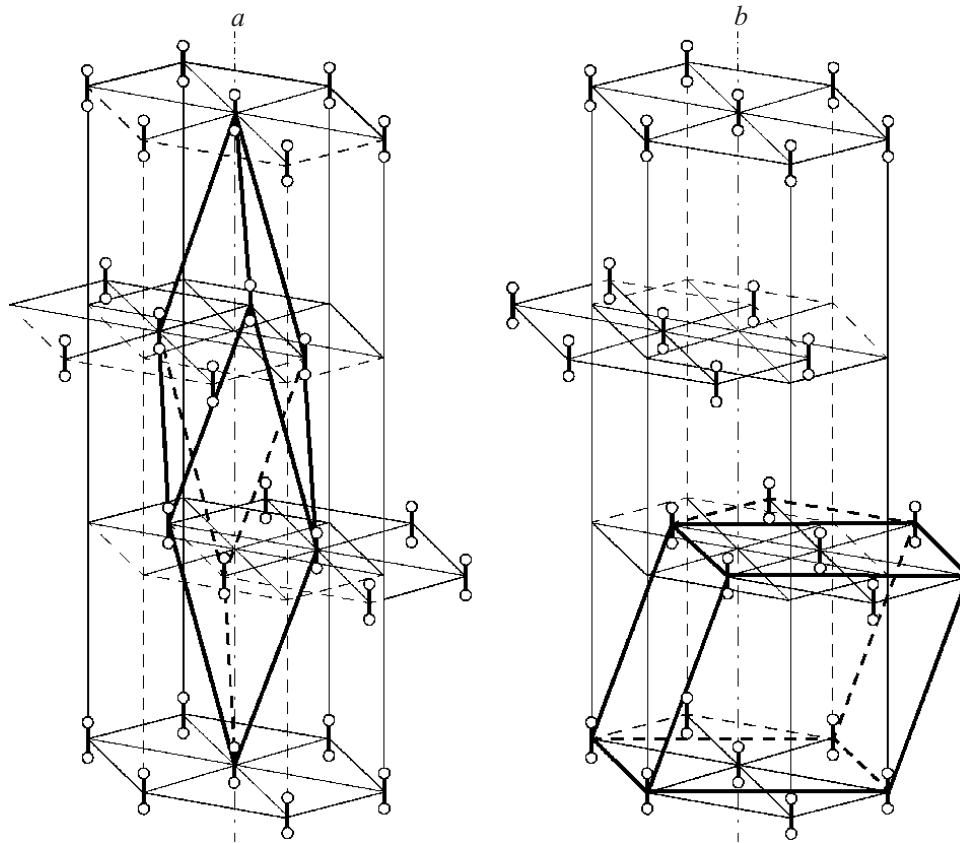


Fig. 2. The structure of  $\beta$ -O<sub>2</sub>. Plotting the crystalline structure in rhombohedral axes (a) in monoclinic axes (b).

As is seen from Fig 2,b, representation of  $\beta$ -phase in monoclinic axis and comparison with  $\alpha$ -phase (Fig. 1) enables to evaluate distortion of crystal lattice of solid oxygen and the disorder antiferromagnetic molecules at the  $\alpha \rightarrow \beta$  transition (Table 1).

As is seen from data of Table 1 and Fig. 4, the  $\alpha \rightarrow \beta$  transition is not connected with changing the orientational structure and the crystal cell undergoes only the distortion

of the basal plane. At this phase transition only the magnetic structure undergoes the changing [1,2]. So the  $\alpha \rightarrow \beta$  transition should be classified most likely as a second-order transition.

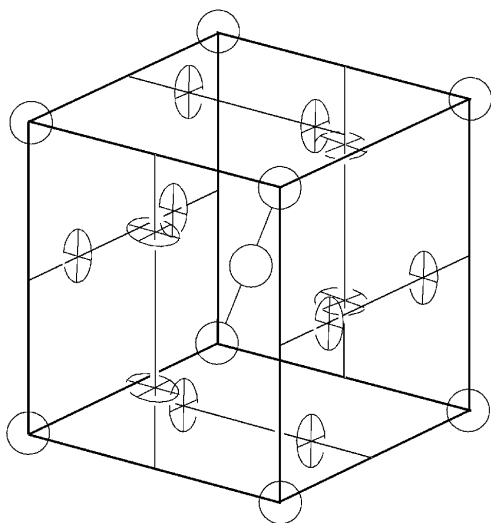


Fig. 3. The structure of  $\gamma$ -O<sub>2</sub>.

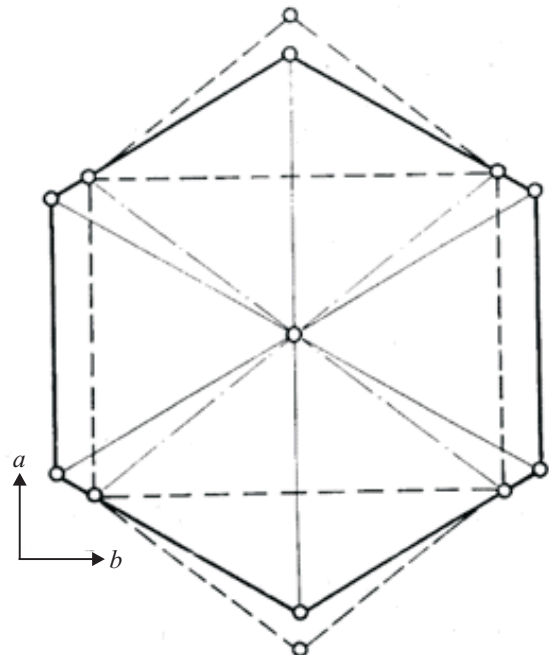


Fig. 4. Plane distortion at the  $\alpha \rightarrow \beta$  transition. The solid line corresponds to  $\beta$ -modification, the dashed line corresponds to  $\alpha$ -modification.

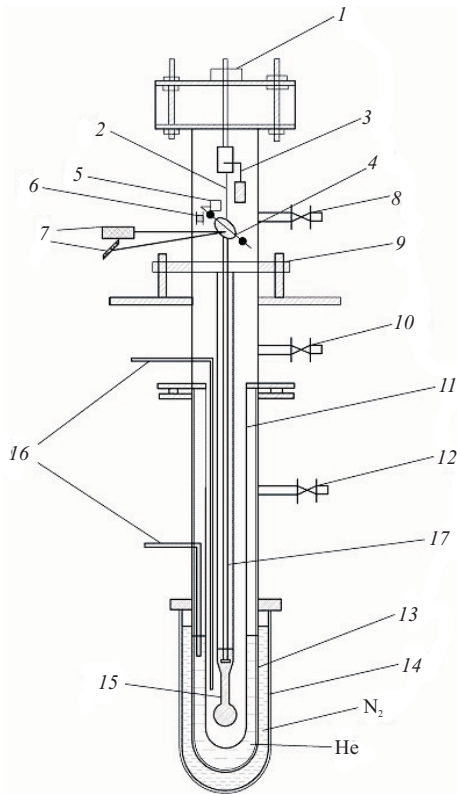


Fig. 5. Schematic of the cryostat for low frequency internal friction measurements in cryocrystals at helium temperatures: suspension regulator for the pendulum (1); suspension wire (2); counterweight (3); internal yoke (4); inductive sensor (5); electromagnet (6); optical system (7); ports for vacuum pumping, admission of gas for study, and helium (8, 10, 12); cryostat mount (9); thermal shield (11); helium dewar; (13); nitrogen dewar (14); sample container (15); helium circulation tubes (16); extension of the internal system of the pendulum (17).

The  $\beta \rightarrow \gamma$  transition, unlike  $\alpha \rightarrow \beta$  one, (Figs. 2,3) is rather crucial for crystal lattice change in both translational

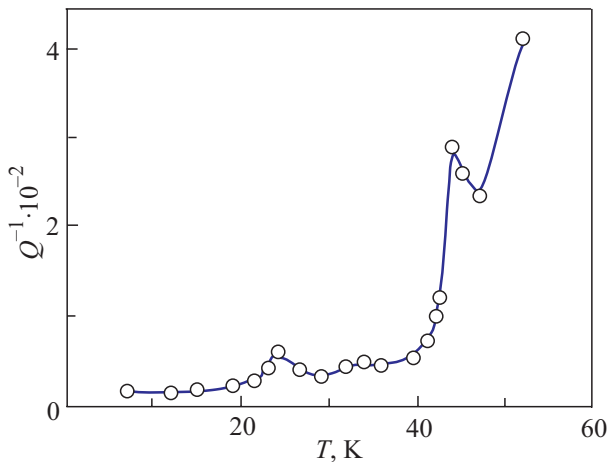


Fig. 6. Temperature dependence of LFIF in polycrystalline oxygen in temperature range 7–52 K.

and orientational structures and corresponds to first-order phase transition. This lattice rearrangement is accompanied by a large volume jump ( $\Delta V/V \approx 4-5\%$  [2]) and latent heat (170 cal/mole [4]) which exceeds the corresponding values even at the melting of the  $\gamma$ -phase at the triple point ( $T_{tr} = 54.36$  K).

The recent paper [4] provides a comprehensive and up-to-date review of the experimental and theoretical literature for solid oxygen. But the results of experimental study of the low frequency internal friction in solid oxygen and anomalies of the temperature dependence of internal friction are not included to this review.

One should note that the temperature dependences of internal friction (IF) of HTSC ceramics at low temperatures are sufficiently influenced by crystalline oxygen into closed pores. So, the IF anomalies near phase transitions in solid oxygen (24 and 44 K) have been reported in the works devoted to high-frequency ( $\approx 100$  kHz) internal friction (HFIF) in the samples of La–Sr and Y–Ba metal-oxide high-Tc superconductors of Varyukhin et al. [5,6] and also in Ref. 7, up to 10 Hz, for low frequency internal friction (LFIF). The same LFIF anomalies have been revealed under the investigations of pure crystalline oxygen. This confirms an assumption about the influence of oxygen in pores on internal friction of HTSC ceramics.

### Experimental technique and results

The cryostat for study of LFIF of solidified gases at temperatures from liquid helium up to room temperatures is shown on Fig. 5. More detail of experimental design was published elsewhere [8].

The LFIF was measured by methods of inverse torsion pendulum under deformation amplitude  $10^{-4}-10^{-5}$  using original setup for study of nonelastic properties of solidified gases [9,10]. An experimental error of LFIF measuring not exceeds 5%.

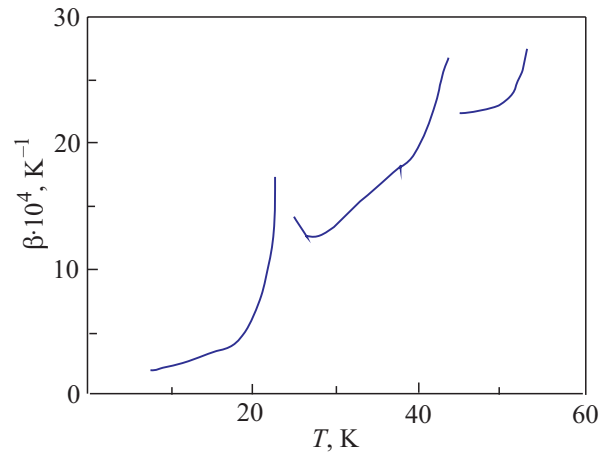


Fig. 7. Temperature dependence of volume thermal expansion coefficient of solid oxygen [2].

The features of preparing of the specimens from various gases were reported in papers [11,12]. Note that an availability of just free specimens (i.e., exfoliated from container walls) has a special interest because of its experimental difficulty. Vapor pressure of oxygen over the specimen surface is sufficiently lower in comparison with other cryocrystals (Ar, Ne, CH<sub>4</sub>, H<sub>2</sub>). Therefore it is necessary to heat the walls of container with specimen up to temperature close to melting point simultaneously with container pumping in order to exfoliate the specimen from the walls. During this process the danger of specimen melting must be avoided.

The unique data on temperature dependence of LFIF  $Q^{-1}(T)$  for crystalline oxygen in temperature range 7–52 K were obtained using free specimens exfoliated from container walls and plotted on Fig. 6. One can see that near temperatures of  $\alpha\beta$ - and  $\beta\gamma$ -phase transitions the LFIF peaks are observed. These peaks greatly differ each from other for the degree of distortion ( $\Delta_{\alpha\beta} \approx 1 \cdot 10^{-2}$  and  $\Delta_{\beta\gamma} \approx 4 \cdot 10^{-2}$ ).

Comparison of temperature dependences of LFIF  $Q^{-1}(T)$  (Fig. 6) with temperature dependences of other thermodynamic properties of solid oxygen (for example, volume expansion coefficient  $\beta(T)$  [2], Fig.7) displays that these anomalies of above thermodynamic features correspond to the temperatures of phase transitions in solid oxygen.

### Conclusions

We studied experimentally the internal friction in temperature range 7–52 K where solid oxygen undergoes a set of  $\alpha$ -,  $\beta$ - and  $\gamma$ -phase. We observed anomalies of the internal friction near the  $\alpha \rightarrow \beta$  and  $\beta \rightarrow \gamma$  phase transitions.

These anomalies of the internal friction can be explained by comparing the temperature dependence of the

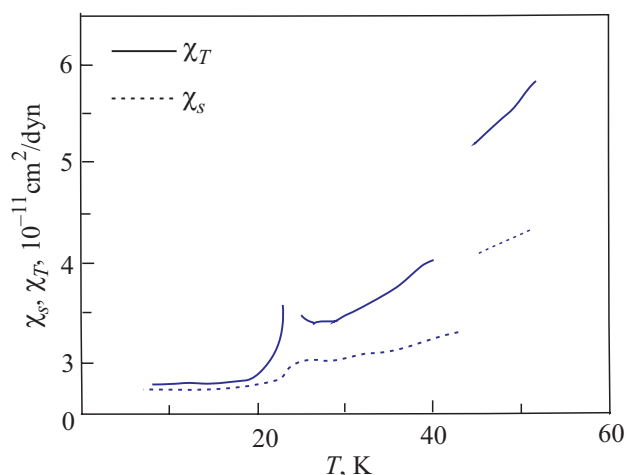


Fig. 8. Temperature dependence of adiabatic ( $\chi_s$ ) and isothermal ( $\chi_T$ ) compressibility of solid oxygen [2]. Calculated  $\chi_s$  values [2] were based on the temperature dependence longitudinal and transverse sound velocities [13–15].

compressibility (Fig. 8) and that of the internal friction (Fig. 6).

Since the internal friction reflects the changing in the elastic-plastic state of solid oxygen, the IF anomalies correlate with the anomalies in the elastic constants and, hence, in the compressibility and are resulted from phase transitions in solid oxygen.

### Acknowledgment

We would like to acknowledge M.A. Strzhemechny for discussion and comments the result of this work.

1. I.A. Burakhovich, I.N. Krupskii, A.I. Prokhvatilov, Yu.A. Freiman, and A.I. Erenburg, *JETP Lett.* **25**, 32 (1977).
2. I.N. Krupskii, A.I. Prokhvatilov, Yu.A. Freiman, and A.I. Erenburg, *Fiz. Nizk. Temp.* **5**, 271 (1979) [*Sov. J. Low Temp. Phys.* **5**, 130 (1979)].
3. A.S. Borovic-Romanov, M.P. Orlova, and P.G. Strelkov, *DAN SSSR* **99**, 699 (1954).
4. Yu.A. Freiman and H.J. Jodl, *Phys. Rep.* **401**, 1 (2004).
5. V.N. Varyukhin A.V. Reznikov, and O.V. Grirut, *Rus. Lett. JETP* **46**, 158 (1987).
6. Yu.A. Burenkov, V.I. Ivanov, A.V. Lebedev, B.L. Baskin, B.K. Kardashev, S.P. Nikanorov, Yu.P. Stepanov, V.G. Fleisher, V.N. Varyukhin, O.I. Datsko, and A.V. Reznikov, *Sov. Phys. Solid State* **30**, 3188 (1988).
7. A.V. Leont'eva, G.A. Marinin, A.Yu. Prokhorov, V.M. Svistunov, B.Ya. Sukharevsky, and L.V. Stepanchuk, *Fiz. Nizk. Temp.* **18**, 705 (1992) [*Low Temp. Phys.* **18**, 489 (1992)].
8. A.V. Leont'eva, G.A. Marinin, and I.A. Oberemchenko, *Fiz. Nizk. Temp.* **10**, 1279 (1984) [*Sov. J. Low Temp. Phys.* **10**, 671 (1984)].
9. G.A. Marinin, A.V. Leont'eva, B.Ya. Sukharevsky, T.N. Anisimova, and Yu.A. Prokhorov, *Fiz. Nizk. Temp.* **11**, 823 (1985) [*Sov. J. Low Temp. Phys.* **11**, 451 (1985)].
10. A.V. Leont'eva, G.A. Marinin, V.M. Svistunov, and B.Ya. Sukharevsky, *Fiz. Nizk. Temp.* **15**, 992 (1989) [*Sov. J. Low Temp. Phys.* **15**, 549 (1989)].
11. G.A. Marinin, A.V. Leont'eva, V.K. Litvinov, and A.Yu. Prokhorov, *Certificate of Recognition № 1587080 (USSR), Inf. Bull. № 31* (1990).
12. A.Yu. Prokhorov, *Rus. Instrum. Exp. Techn.* **6**, 137 (1997).
13. P.A. Bezuglyi, L.M. Tarasenko, and Yu.S. Ivanov, *Sov. Solid State Phys.* **10**, 2119 (1968).
14. P.A. Bezuglyi and L.M. Tarasenko, *Fiz. Nizk. Temp.* **1**, 1144 (1975) [*Sov. J. Low Temp. Phys.* **1**, 548 (1975)].
15. P.A. Bezuglyi, L.M. Tarasenko, and N.Ya. Pushkar, *Proc. Intern. Conf. LT-19, Minsk* (1976), p. 753.